THE JOURNAL OF PHYSICAL CHEMISTRY C

Article

Cite This: J. Phys. Chem. C 2019, 123, 7366−7375

pubs.acs.org/JPCC

Study of Electron-Vibrational Interaction in Molecular Aggregates Using Mean-Field Theory: From Exciton Absorption and Luminescence to Exciton-Polariton Dispersion in Nanofibers

Published as part of The Journal of Physical Chemistry virtual special issue "Abraham Nitzan Festschrift".

Boris D. Fainberg*

Faculty of Sciences, Holon Institute of Technology, 52 Golomb Street, Holon 58102, Israel

School of Chemistry, Tel Aviv University, Tel Aviv 69978, Israel

Supporting Information

ABSTRACT: We developed a model to account for electron-vibrational effects on absorption, luminescence of molecular aggregates, and exciton-polaritons in nanofibers. The model generalizes the mean-field electron-vibrational theory developed by us earlier to the systems with spatial symmetry, exciton luminescence, and the exciton-polaritons with spatial dispersion. The correspondence between manifestation of electron-vibrational interaction in monomers, molecular aggregates, and exciton-polariton dispersion in nanofibers is obtained by introducing the aggregate line-shape functions in terms of the monomer line-shape functions. With the same description of material parameters we calculated both the absorption and luminescence of molecular aggregates and the exciton-polariton dispersion in nanofibers. We apply the theory to experiment on fraction of a millimeter propagation of Frenkel exciton-polaritons in photoexcited organic nanofibers made of thiacyanine dye.

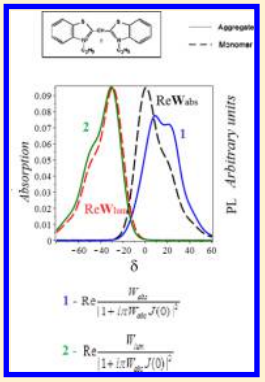

1. INTRODUCTION

The emission of light by Frenkel excitons in organic excitonic materials, for example, dye molecules, polymers, and biological structures including bioinspired peptide beta sheet nanostructures, is used in many photonic applications, including wave guiding, lasers, etc.[1−15] Frenkel excitons are formed by the Coulomb interaction between molecules, so that in the majority of cases photoemission from excitons is accompanied by the exciton annihilation and the photon creation, where two (quasi-) particles (exciton and photon) can be considered separately. In contrast, in ordered materials with large oscillator strength possessing strong absorption, excitons that determine the medium polarization and photons (transverse field) are strongly coupled forming new elementary excitations: polaritons.[10,11,16,17] Exciton-polaritons (EPs) possess properties of both light and matter. Cavity EPs have a mass thanks to their excitonic part that enables us to consider them as an interacting Bose gas[18] leading to Bose−Einstein condensation.[19] The latter results in macroscopic coherence of the condensate and superfluidity.[20] In addition, polariton condensation enables us to realize low threshold polariton lasing without population inversion achieved with conventional nanosecond excitation.[9] Recently topological insulators in EP systems organized as a lattice of coupled semiconductor microcavities in magnetic field were suggested[21,22] and implemented.[23]

Furthermore, electron-vibrational interactions in molecular systems have a pronounced effect on EPs resulting in, among other things, decay and their instability. One way of taking the decay into account is the introduction of complex frequencies with the imaginary part describing phenomenologically constant damping rates (Markovian relaxation).[24,25] In general, taking the effect of strong electron-vibrational interactions on the EPs into account is a nontrivial problem. The point is that in this case both the interaction with radiation field and electron-vibrational interaction should be considered as strong.[26] La Rocca et al.[25,27] studied polariton dispersion in organic-based microcavities taking a single high-frequency (HF) optically active (OA) intramolecular vibration into account introducing also complex exciton replicas frequencies (see above).

However, in real situations the relaxation of molecular and excitonic systems is non-Markovian and cannot be described using constant decay rates resulting in the Lorentzian shape of spectra. Using such a description, one may simulate a separate spectrum of an exciton[6] or even polaritonic luminescence[3] using fitting parameters, but one cannot describe the transformation of spectra when, for example, monomers form an aggregate, etc.[28] (see also ref 29). The matter is that if the monomer spectrum has Lorentzian shape, the aggregate spectrum is simply shifted monomer spectrum.[28] At the same time, other shapes that non-Markovian theory leads to

Received: January 20, 2019
Revised: February 22, 2019
Published: February 22, 2019

DOI: 10.1021/acs.jpcc.9b00582
J. Phys. Chem. C 2019, 123, 7366−7375

are able to describe the transformation of spectra including strong narrowing the J-aggregate absorption spectrum with respect to that of a monomer.[28]

It is worth noting that actual dissipative properties of the vibrational system are very important for EPs, in particular, for EP fluorescence propagating in organic nanofibers.[3] The point is that a "blue" part of the fluorescence spectrum overlaps with the wing of the imaginary part of the wavenumber defining absorption and, therefore, is partly absorbed.[3,28]

In ref 28 we developed a mean-field electron-vibrational theory of Frenkel EPs in organic dye structures and applied it to the aggregate absorption and the experiment on long-range polariton propagation in organic dye nanofibers at room temperature.[3,4] The theory is non-Markovian and is able to describe the transformation of absorption spectra on molecular aggregation. In the present work we generalize the theory developed in ref 28 to the systems with spatial symmetry (like organic molecular crystals), to the exciton luminescence and the exciton-polaritons with spatial dispersion. The matter is that ordered structures also include, among other things, organic dye nanofibers[1,3] that are synthesized by self-assembly of thiacyanine (TC) dye molecules in solution. We obtain the correspondence between manifestation of electron-vibrational interaction in monomers, molecular aggregates, and exciton-polaritons in nanofibers. With the same description of material parameters we calculate both the absorption and luminescence of molecular aggregates and the exciton-polariton dispersion in nanofibers. We apply the theory to experiment on fraction of a millimeter propagation of Frenkel exciton polaritons in photoexcited organic nanofibers made of TC dye.[3,4]

The paper is organized as follows. We start with the derivation of the mean-field equations in ordered structures taking electron-vibrational and dipole−dipole intermolecular interactions in condensed matter into account. Then we solve these equations in the momentum representation, Section 2.1. In Section 3 we calculate polarization, susceptibility, and dielectric function in the **k** space. In Section 4 we calculate the relaxed luminescence of aggregates for weak excitation. The exciton luminescence and absorption spectra in our mean-field theory obey Stepanov's law.[11,30] Our theory describes both narrowing the J-aggregate absorption and luminescence spectra, and diminishing the Stokes shift between them with respect to that of a monomer. In Section 5 we apply the theory to experiment on fraction of a millimeter propagation of EPs in photoexcited fiber-shaped H-aggregates of TC dye at room temperature[3] bearing in mind the correspondence between manifestation of electron-vibrational interaction in monomers, molecular aggregates, and EP dispersion in nanofibers, and in Section 6, we briefly conclude.

2. DERIVATION OF EQUATIONS FOR EXPECTATION VALUE OF EXCITONIC OPERATOR IN ORDERED STRUCTURES

In this section we shall consider an ensemble of molecules with two electronic states $n = 1$ (ground) and 2 (excited) in a condensed matter described by the exciton Hamiltonian

$$H_{\text{exc}} = H_0 + H_{\text{int}} \tag{1}$$

Here the molecular Hamiltonian, H_0, is given by

$$H_0 = \sum_{j=1}^{2} [E_j + W_j(\mathbf{Q})] \sum_m |mj\rangle\langle mj| \tag{2}$$

where $E_2 > E_1$, E_j is the energy of state j, and $W_j(\mathbf{Q})$ is the adiabatic Hamiltonian of the vibrational subsystem of a molecule interacting with the two-level electron system under consideration in state j. The dipole−dipole intermolecular interactions in the condensed matter are described by the interaction Hamiltonian[31,32]

$$H_{\text{int}} = \hbar \sum_m \sum_{n\neq m} J_{mn} b_m^\dagger b_n \tag{3}$$

where J_{mn} is the resonant exciton coupling, $b_m = |m1\rangle\langle m2|$ is the operator that describes the annihilation of an excitation in molecule m at level 2, and $b_m^\dagger = |m2\rangle\langle m1|$ is the operator that describes the creation of an excitation of molecule m to level 2. We adopt here the Coulomb gauge for the electromagnetic field, according to which the Coulomb interaction between molecules is conditioned by the virtual scalar and longitudinal photons.[11,31] In addition, the interaction conditioned by the transverse photons exists, quantum electromagnetic field $\hat{\mathbf{E}}(t)$

$$\hat{\mathbf{E}}(\mathbf{r}, t) = \frac{1}{2}\left\{ \sum_{\mathbf{q}} \mathbf{e}_{\mathbf{q}} \mathcal{E}_{\mathbf{q}} \exp[i(\mathbf{q}\cdot\mathbf{r} - \omega_{\mathbf{q}} t)] + \text{h. c.} \right\} \tag{4}$$

Then the system Hamiltonian takes the form

$$H = H_{\text{exc}} + \hbar \sum_{\mathbf{q}} \omega_{\mathbf{q}} a_{\mathbf{q}}^\dagger a_{\mathbf{q}} - \hat{\mathbf{D}}\cdot\hat{\mathbf{E}} \tag{5}$$

Here $\mathbf{e}_{\mathbf{q}}\mathcal{E}_{\mathbf{q}}\exp(i\mathbf{q}\cdot\mathbf{r}) = i2\sqrt{2\pi\hbar\omega_{\mathbf{q}}}\, a_{\mathbf{q}} u_{\mathbf{q}}(\mathbf{r})$ is the field amplitude, $a_{\mathbf{q}}$ is the annihilation operator for mode $\mathbf{q}$, $\mathbf{e}_{\mathbf{q}}$ is the unit photon polarization vector, V is the photon quantization volume, $u_{\mathbf{q}}(\mathbf{r})$ describes a space dependence of the field amplitude, where $u_{\mathbf{q}}(\mathbf{r}) = \mathbf{e}_{\mathbf{q}} \exp(i\mathbf{q}\cdot\mathbf{r})V^{-1/2}$ for plane waves, and $\hat{\mathbf{D}}$ is the dipole moment operator of a molecule. The latter can be written as $\hat{\mathbf{D}} = \mathbf{D}\sum_m (b_m + b_m^\dagger)$ with $\mathbf{D}$ the electronic transition dipole moment. It is worth noting that, if one wants to introduce photons in a cavity, one uses the cavity eigenmodes for the expansion instead of plane waves.

Among other things the interaction, the term "$-\hat{\mathbf{D}}\cdot\hat{\mathbf{E}}$" is responsible for the creation of EPs. In an experiment related to a linear absorption by excitons one can consider the electromagnetic field classically. In that case one can use the same formula 4 considering $\mathbf{E}(\mathbf{r},t)$ and $\mathcal{E}_{\mathbf{q}}$ as classical function. In this work we also consider a luminescence experiment, where the electromagnetic field may be decomposed into two modes, namely, classical (incoming field) and quantum (the scattered field mode generated by spontaneous emission), eq 4. In any case, the field frequency, $\omega_{\mathbf{q}}$, is close to that of the transition $1 \rightarrow 2$.

Consider structures that are symmetric in space like organic molecular crystals. Such structures include also organic dye nanofibers[1,3] that are synthesized by self-assembly of TC dye molecules in solution.

We define the exciton annihilation $b_{\mathbf{k}}$ and creation $b_{\mathbf{k}}^\dagger$ operators in the momentum representation[11,31]

$$b_{\mathbf{k}} = \frac{1}{\sqrt{N}} \sum_m b_m \exp(-i\mathbf{k}\cdot\mathbf{r}_m) \tag{6}$$

$$b_{\mathbf{k}}^\dagger = \frac{1}{\sqrt{N}} \sum_m b_m^\dagger \exp(i\mathbf{k}\cdot\mathbf{r}_m) \tag{7}$$

and the lattice Fourier transform of intermolecular interaction[10,11,17]

DOI: 10.1021/acs.jpcc.9b00582
J. Phys. Chem. C 2019, 123, 7366−7375

$$J(\mathbf{k}) = \sum_{n\neq m} J_{mn} \exp[i\mathbf{k}\cdot(\mathbf{r}_n - \mathbf{r}_m)]) \tag{8}$$

where $\mathcal{N}$ is the number of interacting molecules. Then

$$b_n = \frac{1}{\sqrt{\mathcal{N}}} \sum_{\mathbf{k}} b_{\mathbf{k}} \exp(i\mathbf{k}\cdot\mathbf{r}_n) \tag{9}$$

Note that $J(0) = \sum_{n\neq m} J_{mn} = -p$, where p is the parameter of intermolecular interaction used in ref 28.

In the absence of vibrations, the unitary transformation, eqs 6, (7), (8), and (9), enables us to diagonalize the electronic part of the excitonic Hamiltonian, H_{exc}, considering $b_{\mathbf{k}}$ as Bose operators

$$b_{\mathbf{k}'}b_{\mathbf{k}}^{\dagger} - b_{\mathbf{k}}^{\dagger}b_{\mathbf{k}'} = \delta_{\mathbf{k}\mathbf{k}'} \tag{10}$$

that is correct for weak excitation. In that case using the Heisenberg equations of motion, one obtains that $\hat{H}_{\mathrm{int}}$ gives the following contribution to the change of the excitonic operator $b_{\mathbf{k}}$ in time

$$\frac{\mathrm{d}}{\mathrm{d}t}b_{\mathbf{k}} \approx \frac{i}{\hbar}[\hat{H}_{\mathrm{int}}, b_{\mathbf{k}}] = -iJ(\mathbf{k})b_{\mathbf{k}} \tag{11}$$

Now let us take the vibrational subsystem of molecules into account. Since an absorption spectrum of a large molecule in condensed matter consists of overlapping vibronic transitions, we shall single out the contribution from the low-frequency (LF) OA vibrations $\{\omega_s\}$ to $W_j(\mathbf{Q})$: $W_j(\mathbf{Q}) = W_{j\mathrm{M}} + W_{js}$, where W_{js} is the Hamiltonian governing the nuclear degrees of freedom of the LFOA molecular vibrations, and $W_{j\mathrm{M}}$ is the Hamiltonian representing the nuclear degrees of freedom of the HFOA vibrations of a molecule.

The influence of the vibrational subsystems of molecule m on the electronic transition within the range of definite vibronic transition related to HFOA vibration (∼1000−1500 cm^{-1}) can be described as a modulation of this transition by LFOA vibrations $\{\omega_s\}$.[33] We suppose that $\hbar\omega_s \ll k_{\mathrm{B}}T$. Thus, $\{\omega_s\}$ is an almost classical system. In accordance with the Franck−Condon principle, an optical electronic transition takes place at a fixed nuclear configuration. Therefore, the quantity $u_{1s}(\mathbf{Q}) = W_{2s}(\mathbf{Q}) - W_{1s}(\mathbf{Q}) - \langle W_{2s}(\mathbf{Q}) - W_{1s}(\mathbf{Q})\rangle_1$ representing electron-vibration coupling is the disturbance of nuclear motion under electronic transition, where $\langle\rangle_j$ stands for the trace operation over the reservoir variables in the electronic state j. Electronic transition relaxation stimulated by LFOA vibrations is described by the correlation function $K_m(t) = \langle\alpha_m(0)\alpha_m(t)\rangle$ of the corresponding vibrational disturbance with characteristic attenuation time τ_s,[32,34,35] where $\alpha_m \equiv -u_{1s}/\hbar$. In other words, LFOA vibrations lead to a stochastic modulation of the frequency of electronic transition 1 → 2 of molecule m according to $\tilde{\omega}_{21}(t) = \omega_{21} - \alpha_m(t)$, where $\omega_{21} = [(E_2 - E_1) + \langle W_{2s}(\mathbf{Q}) - W_{1s}(\mathbf{Q})\rangle_1]/\hbar$ is the frequency of Franck−Condon transition 1 → 2, and $\alpha_m(t)$ is assumed to be Gaussian-Markovian process with $\langle\alpha_m(t)\rangle = 0$ and exponential correlation function $K_m(t) = K(t) = K(0)\exp(-|t|/\tau_s)$. For brevity, we consider first a single vibronic transition related to a HFOA vibration. Generalization to the case of a number of vibronic transitions with respect to a HFOA vibration will be made later.

Consider the expectation value of excitonic operator b_m

$$\langle b_m(\alpha)\rangle \equiv Tr[b_m\rho_m(\alpha, t)] \tag{12}$$

where $\rho_{m,ij}(\alpha,t)$ is the partial density matrix of molecule m.[28,36,37] Diagonal elements of the density matrix $\rho_{m,jj}(\alpha,t)$ describe the molecule distribution in states 1 and 2 with a given value of α at time t. The complete density matrix averaged over the stochastic process, which modulates the molecule energy levels, is obtained by integration of $\rho_{m,ij}(\alpha,t)$ over α, $\langle\rho_m\rangle_{ij}(t) = \int\rho_{m,ij}(\alpha,t)\,\mathrm{d}\alpha$, where quantities $\langle\rho_m\rangle_{jj}(t)$ are the normalized populations of the corresponding electronic states: $\langle\rho_m\rangle_{jj}(t) \equiv n_{m,j}$, $n_{m,1} + n_{m,2} = 1$. Combining eqs 6 and (12), one can introduce the expectation value of $b_{\mathbf{k}}$

$$\langle b_{\mathbf{k}}(\alpha)\rangle = \frac{1}{\sqrt{\mathcal{N}}} \sum_m \langle b_m(\alpha)\rangle\exp(-i\mathbf{k}\cdot\mathbf{r}_m) \tag{13}$$

where $\langle b_m(\alpha)\rangle = \rho_{m,21}(\alpha,t)$,[28,38] and averaging in the density matrix is performed with respect to the vibrational subsystem of the mth molecule.

Let us write the equation for the expectation value of $b_{\mathbf{k}}$ corresponding to operator eq 11. If one considers only intramolecular vibrations, $\hat{H}_{\mathrm{int}}$ gives the following contribution to the change of the expectation value of excitonic operator b_m in time in the site representation[28]

$$\begin{aligned}\frac{\partial}{\partial t}\langle b_m(\alpha)\rangle &\approx \frac{i}{\hbar}\langle[\hat{H}_{\mathrm{int}}, b_m]\rangle \\ &\equiv \frac{i}{\hbar}Tr([\hat{H}_{\mathrm{int}}, b_m]\rho) \\ &= -i\sum_{n\neq m} J_{mn}\langle\hat{n}_{m1}(\alpha) - \hat{n}_{m2}(\alpha)\rangle\langle b_n\rangle\end{aligned} \tag{14}$$

where $\hat{n}_{m1} = b_m b_m^{\dagger}$, $\hat{n}_{m2} = b_m^{\dagger}b_m$ is the exciton population operator, $\langle n_{m1}(\alpha)\rangle = \rho_{m,11}(\alpha,t)$, and $\langle n_{m2}(\alpha)\rangle = \rho_{m,22}(\alpha,t)$ may be neglected for weak excitation. Here $\langle b_n\rangle = \int\langle b_n(\alpha)\rangle d\alpha = \int\rho_{n,21}(\alpha,t)\,\mathrm{d}\alpha$ is the complete density matrix averaged over the stochastic process.

We emphasize that factorization adopted in eq 14 corresponded to neglect of all correlations among different molecules.[28] At the same time the factorization corresponds to a random phase approximation[39] that enables us to split the term $\langle(\hat{n}_{m1} - \hat{n}_{m2})b_n\rangle$ into the product of populations and polarization ($\langle b_n\rangle$). It is in this sense that the factorization can be understood in the momentum representation.

Furthermore, neglecting $b_{\mathbf{k}}^{\dagger}b_{\mathbf{k}'}$ in eq 10 for weak excitation, one can write $b_{\mathbf{k}'}b_{\mathbf{k}}^{\dagger} \simeq \delta_{\mathbf{k}\mathbf{k}'}$ or

$$b_{\mathbf{k}'}b_{\mathbf{k}}^{\dagger} - b_{\mathbf{k}}^{\dagger}b_{\mathbf{k}'} \simeq \hat{n}_{1\mathbf{k}}\delta_{\mathbf{k}\mathbf{k}'} \tag{15}$$

where $\hat{n}_{1\mathbf{k}} \simeq 1$. Using eq 14 and eqs 6, (7), (8), (9), (13), and (15), we get

$$\frac{\partial}{\partial t}\langle b_{\mathbf{k}}(\alpha)\rangle \approx -iJ(\mathbf{k})\langle b_{\mathbf{k}}\rangle\rho_{11}^{(0)}(\alpha) \tag{16}$$

where $\langle b_{\mathbf{k}}\rangle = \int\langle b_{\mathbf{k}}(\alpha)\rangle d\alpha$ and $\rho_{11}^{(0)}(\alpha)$ is the equilibrium value of $\rho_{11}(\alpha)$.

Equation 16 describes the contribution of $\hat{H}_{\mathrm{int}}$ to the change of the expectation value $\langle b_{\mathbf{k}}(\alpha)\rangle$ in time in the momentum representation. In addition, the change of $\langle b_{\mathbf{k}}(\alpha)\rangle$ is determined by the vibrational relaxation. If one considers an absorption experiment and the corresponding polariton problem, the relevant vibrational relaxation occurs in the ground electronic state. In that case the density matrix of a monomer molecule $\rho_{m,21}(\alpha,t) = \langle b_m(\alpha)\rangle$ obeys the equation[28,36,37,40−42]

DOI: 10.1021/acs.jpcc.9b00582
J. Phys. Chem. C 2019, 123, 7366−7375

$$\left[\frac{\partial}{\partial t} + i(\omega_{21} - \alpha) - L_{11}\right]\rho_{m,21}(\alpha, t) = \frac{i}{2\hbar}\mathbf{D}_{21}\cdot\mathbf{e}_{\mathbf{q}}\mathcal{E}_{\mathbf{q}}\exp[i(\mathbf{q}\cdot\mathbf{r}_m - \omega_{\mathbf{q}}t)]\rho^{(0)}_{m,11}(\alpha) \quad (17)$$

where operator

$$L_{11} = \tau_s^{-1}\left[1 + \alpha\frac{\partial}{\partial\alpha} + K(0)\frac{\partial^2}{\partial\alpha^2}\right] \quad (18)$$

describes the diffusion with respect to coordinate α in the effective parabolic potential $U_1(\alpha)$.

Bearing in mind that $\langle b_m(\alpha)\rangle = \rho_{m,21}(\alpha,t)$, we multiply both sides of eq 17 by $\exp(-i\mathbf{k}\cdot\mathbf{r}_m)$ and sum with respect to m. As a result we get

$$\left[\frac{\partial}{\partial t} + i(\omega_{21} - \alpha) - L_{11}\right]\langle b_{\mathbf{k}}(\alpha)\rangle = \frac{i}{2\hbar}\sqrt{N}\mathbf{D}_{21}\cdot\mathbf{e}_{\mathbf{k}}\mathcal{E}_{\mathbf{k}}\exp(-i\omega_{\mathbf{k}}t)\rho^{(0)}_{11}(\alpha) \quad (19)$$

where we used formula $\sum_m \exp[i(\mathbf{q} - \mathbf{k})\cdot\mathbf{r}_m] = N\delta_{\mathbf{qk}}$.[11,31]

Combining eqs 16 and (19), we finally get

$$\left[\frac{\partial}{\partial t} + i(\omega_{21} - \alpha) - L_{11}\right]\langle b_{\mathbf{k}}(\alpha)\rangle = i\left[\frac{\sqrt{N}}{2\hbar}\mathbf{D}_{21}\cdot\mathbf{e}_{\mathbf{k}}\mathcal{E}_{\mathbf{k}}\exp(-i\omega_{\mathbf{k}}t) - J(\mathbf{k})\langle b_{\mathbf{k}}\rangle\right]\rho^{(0)}_{11}(\alpha) \quad (20)$$

2.1. Solution of eq 20. Consider first the slow modulation limit when $K(0)\tau_s^2 \gg 1$. In that case the term L_{11} on the left-hand side of eq 20 can be discarded,[28,37,41] and we get

$$\frac{\partial}{\partial t}\langle\tilde{b}_{\mathbf{k}}(\alpha)\rangle = -i(\omega_{21} - \omega_{\mathbf{k}} - \alpha)\langle\tilde{b}_{\mathbf{k}}(\alpha)\rangle + i\left[\frac{\sqrt{N}}{2\hbar}\times\mathbf{D}_{21}\cdot\mathbf{e}\mathcal{E}_{\mathbf{k}} - J(\mathbf{k})\langle\tilde{b}_{\mathbf{k}}\rangle\right]\rho^{(0)}_{11}(\alpha) \quad (21)$$

where $\langle\tilde{b}_{\mathbf{k}}(\alpha)\rangle = \langle b_{\mathbf{k}}(\alpha)\rangle\exp(i\omega_{\mathbf{k}}t)$. In the steady-state regime, eq 21 leads to

$$\langle\tilde{b}_{\mathbf{k}}\rangle = \frac{i\pi W_a(\omega_{\mathbf{k}})\frac{\sqrt{N}}{2\hbar}\mathbf{D}_{21}\cdot\mathbf{e}\mathcal{E}_{\mathbf{k}}}{1 + i\pi W_a(\omega_{\mathbf{k}})J(\mathbf{k})} \quad (22)$$

where

$$W_a(\omega_{\mathbf{k}}) = i\int_{-\infty}^{\infty} d\alpha\rho^{(0)}_{11}\zeta(\omega_{\mathbf{k}} - \omega_{21} + \alpha)/\pi \quad (23)$$

is the monomer spectrum, $\zeta(\omega_{\mathbf{k}} - \omega_{21} + \alpha) = \frac{P}{\omega_{\mathbf{k}} - \omega_{21} + \alpha} - i\pi\delta(\omega_{\mathbf{k}} - \omega_{21} + \alpha)$, P is the symbol of the principal value. The imaginary part of "$-iW_a(\omega_{\mathbf{k}})$" with sign minus, $-\mathrm{Im}[-iW_a(\omega_{\mathbf{k}})] = \mathrm{Re}W_a(\omega_{\mathbf{k}}) \equiv F_a(\omega_{\mathbf{k}})$, describes the absorption line shape of a monomer molecule, and the real part, $\mathrm{Re}[-iW_a(\omega_{\mathbf{k}})] = \mathrm{Im}W_a(\omega_{\mathbf{k}})$, describes the corresponding refraction spectrum. For the "slow modulation" limit, quantities $W_a(\omega_{\mathbf{k}})$ and $F_a(\omega_{\mathbf{k}})$ are given by

$$W_a(\omega_{\mathbf{k}}) = \sqrt{\frac{1}{2\pi K(0)}}\,w\left(\frac{\omega_{\mathbf{k}} - \omega_{21}}{\sqrt{2K(0)}}\right) \quad (24)$$

where $w(z) = \exp(-z^2)[1 + i\mathrm{erfi}(z)]$ is the probability integral of a complex argument,[43] and

$$F_a(\omega_{\mathbf{k}}) = \sqrt{\frac{1}{2\pi K(0)}}\exp\left[-\frac{(\omega_{21} - \omega_{\mathbf{k}})^2}{2K(0)}\right] \quad (25)$$

It might be well to point out that the magnitude $W_a(\omega_{\mathbf{k}})$ is proportional to the molecular polarizability, and the expression in the square brackets on the right-hand side of eq 21 may be considered as the interaction with the local field in the $\mathbf{k}$-space divided by $\hbar$. Therefore, eq 22 can be used also beyond the slow modulation limit, when $W_a(\omega_{\mathbf{k}})$ is given by[40,44] (see Section 1 of the Supporting Information)

$$W_a(\omega_{\mathbf{k}}) = \frac{\tau_s}{\pi}\frac{\Phi(1, 1 + x_a; K(0)\tau_s^2)}{x_a} \quad (26)$$

where $x_a = K(0)\tau_s^2 + i\tau_s(\omega_{21} - \omega_{\mathbf{k}})$, $\Phi(1,1 + x_a; K(0)\tau_s^2)$ is a confluent hypergeometric function.[43] In that case one cannot neglect the term L_{11} describing relaxation in the ground electronic state (see Section 1 of the Supporting Information). In this relation one should note the following. The "slow modulation" limit, eqs 24 and (25), is correct only near the absorption maximum. The wings decline much slower as $(\omega_{21} - \omega_{\mathbf{k}})^{-4}$.[40] At the same time, the expression for $\langle\tilde{b}_{\mathbf{k}}\rangle$, eq 22, has a pole, giving strong increasing $\langle\tilde{b}_{\mathbf{k}}\rangle$, when $1/[J(\mathbf{k})\pi] = \mathrm{Im}W_a(\omega_{\mathbf{k}})$. If parameter of the dipole−dipole intermolecular interaction $|J(\mathbf{k})|$ is rather large, the pole may be at a large distance from the absorption band maximum, where the "slow modulation" limit breaks down. This means one should use exact expression for the monomer spectrum W_a that is not limited by the "slow modulation" approximation and properly describes both the central spectrum region and its wings.[28] Equation 26 is the exact expression for the Gaussian−Markovian modulation with the exponential correlation function $K(t) = K(0)\exp(-|t|/\tau_s)$.

Moreover, we can take also HFOA intramolecular vibrations into account, in addition to the LFOA vibrations $\{\omega_s\}$ discussed thus far. In that case $W_a(\omega_{\mathbf{k}})$ is given by[28] (see Section 2 of the Supporting Information)

$$W_a(\omega_{\mathbf{k}}) = \frac{\tau_s}{\pi}\exp(-S_0\coth\theta_0)\sum_{l=-\infty}^{\infty} I_l\left(\frac{S_0}{\sinh\theta_0}\right)\times\exp(l\theta_0)\frac{\Phi(1, 1 + x_{al}; K(0)\tau_s^2)}{x_{al}} \quad (27)$$

where $x_{al} = K(0)\tau_s^2 + i\tau_s(\omega_{21} - \omega_{\mathbf{k}} + l\omega_0)$. We consider one normal HF intramolecular oscillator of frequency ω_0 whose equilibrium position is shifted under electronic transition, and S_0 is the dimensionless parameter of the shift, $\theta_0 = \hbar\omega_0/(2k_BT)$, $I_l(x)$ is the modified Bessel function of first kind.[43]

Equation 27 is the extension of eq 26 to the presence of the HFOA intramolecular vibrations. For $\theta_0 \gg 1$ we obtain

$$W_a(\omega_{\mathbf{k}}) = \frac{\tau_s}{\pi}\exp(-S_0)\sum_{l=0}^{\infty}\frac{S_0^l}{l!}\frac{\Phi(1, 1 + x_{al}; K(0)\tau_s^2)}{x_{al}} \quad (28)$$

3. POLARIZATION, SUSCEPTIBILITY, AND DIELECTRIC FUNCTION IN K-SPACE

The positive frequency component of the polarization per unit volume at point $\mathbf{r}$ can be written as

DOI: 10.1021/acs.jpcc.9b00582
J. Phys. Chem. C 2019, 123, 7366−7375

$$\mathbf{P}^{+}(\mathbf{r}, t) = N\mathbf{D}_{12}\langle b_m\rangle = \mathbf{P}(\mathbf{k}, \omega_{\mathbf{k}})\exp[i(\mathbf{k}\cdot\mathbf{r} - \omega_{\mathbf{k}}t)] \tag{29}$$

where

$$\mathbf{P}(\mathbf{k}, \omega_{\mathbf{k}}) = N\mathbf{D}_{12}\frac{1}{\sqrt{N}}\langle\tilde{b}_{\mathbf{k}}\rangle = \frac{N\mathbf{D}_{12}}{2\hbar}\frac{i\pi W_a(\omega_{\mathbf{k}})\mathbf{D}_{21}\cdot\mathbf{e}_{\mathbf{k}}\mathcal{E}_{\mathbf{k}}}{1 + i\pi W_a(\omega_{\mathbf{k}})J(\mathbf{k})} \tag{30}$$

N is the density of molecules, and we used eqs 9 and (22).

Knowing $\mathbf{P}(\mathbf{k},\omega_{\mathbf{k}})$, one can calculate the susceptibility

$$\chi(\mathbf{k}, \omega_{\mathbf{k}}) = \frac{N\mathbf{D}_{12}\mathbf{D}_{21}}{\hbar}\frac{i\pi W_a(\omega_{\mathbf{k}})}{1 + i\pi W_a(\omega_{\mathbf{k}})J(\mathbf{k})} \tag{31}$$

and the dielectric function $\varepsilon(\mathbf{k},\omega_{\mathbf{k}}) = \varepsilon_0[1 + 4\pi\chi(\mathbf{k},\omega_{\mathbf{k}})]$[39]

$$\varepsilon(\mathbf{k}, \omega_{\mathbf{k}}) = \varepsilon_0\left[1 + 4\pi\frac{N\mathbf{D}_{12}\mathbf{D}_{21}}{\hbar}\frac{i\pi W_a(\omega_{\mathbf{k}})}{1 + i\pi W_a(\omega_{\mathbf{k}})J(\mathbf{k})}\right] \tag{32}$$

where $\varepsilon_0 = n_0^2$, n_0 is the background refractive index of the medium, and the vector product in the numerator of eqs 31 and (32) is a dyadic product.

If we assume for simplicity that the excitons have an isotropic effective mass, then

$$J(\mathbf{k}) = J(0) + \frac{\hbar\mathbf{k}^2}{2m^*} \tag{33}$$

where the exciton effective mass, m^*, may be both positive and negative. One can see that the susceptibility, eq 31, has a pole when the imaginary part of the monomer spectrum, $\mathrm{Im}W_a(\omega_{\mathbf{k}})$, is equal to $1/[J(\mathbf{k})\pi]$, that is, at the frequency of the exciton with the same wave vector as the exciting field. In other words, we deal with spatial dispersion. It is worth noting that the structure of the dispersion curves $J(\mathbf{k})$ occurs on the scale of $|\mathbf{k}| \approx (0.1{-}1\ \mathrm{nm})^{-1}$, which is much larger than the scale of an optical wave vector. For this reason in practice one may often neglect the spatial dispersion and simply calculate the exciton resonances for $J(0)$, as we did in ref 28 and where we obtained a good agreement between theoretical and experimental absorption spectra of H-aggregates. In contrast, spatial dispersion may be of importance for J-aggregates, due to small bandwidth of their spectra, and also in microcavities, where the exciton effective mass may be much smaller than electron mass,[11] and then the second term on the right-hand side of eq 33 strongly increases. Figure 1 shows the absorption spectra of a J-aggregate that are proportional to the imaginary part of the susceptibility $\mathrm{Re}\frac{W_a(\omega_{\mathbf{k}})}{1 + i\pi W_a(\omega_{\mathbf{k}})J(\mathbf{k})}$, eq 33, calculated for $J(\mathbf{k}) = J(0)$[28] (solid line), and for $J(\mathbf{k}) = J(0) + \frac{\hbar\mathbf{k}^2}{2m^*}$ (dashed line). The monomer spectrum $W_a(\omega_{\mathbf{k}})$ is calculated using eq 26. One can see that, due to small bandwidth of the J-aggregate absorption with respect to that of the monomer (see Figure 1 of ref 28), the spatial dispersion can lead to marked broadening of the J-aggregate spectrum. In contrast, the role of the spatial dispersion may be overestimated in works not considering the vibrational contribution.[3,45]

4. LUMINESCENCE

In this section we shall use our mean-field theory for the calculation of the relaxed luminescence of aggregates for weak excitation. To describe this process, we shall consider a quantum electromagnetic field of the spontaneous emission

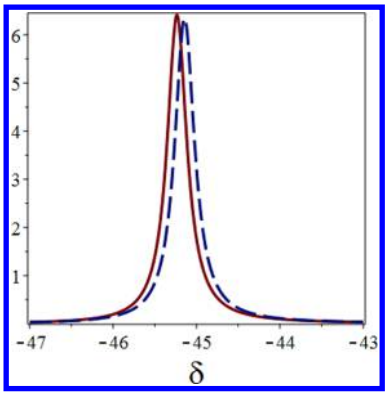

Figure 1. Absorption spectra (in terms of τ_s/π) of a J-aggregate calculated for $J(\mathbf{k}) = J(0)$ (solid line), and $J(\mathbf{k}) = J(0) + \frac{\hbar\mathbf{k}^2}{2m^*}$ (dashed line) in the case of slow modulation ($\sqrt{K(0)}\tau_s = 10.9 > >1$) and $-J(0)\tau_s = 42$. Dimensionless parameter is $\delta = \tau_s(\omega_{\mathbf{k}} - \omega_{21})$. Other parameters are $m^* = 0.1m_{el}$, m_{el} is the electron mass, $|\mathbf{k}| = n2\pi/\lambda$, $n = 3.16$ is the refraction index, $\lambda = 0.5\ \mu$.

$$\mathbf{E}_s(\mathbf{r}, t) = \frac{1}{2}\mathbf{e}_s\mathcal{E}_s\exp(\mathbf{k}_s\mathbf{r} - i\omega_s t) + \frac{1}{2}\mathbf{e}_s^*\mathcal{E}_s^{\dagger}\exp(\mathbf{k}_s\mathbf{r} - i\omega_s t) \tag{34}$$

in addition to the incident classical field of frequency ω. Equation 34 is eq 4 for $\mathbf{q} = \mathbf{k}_s$. This process is depicted by the double-sided Feynman diagrams,[32,41,46] where due to condensed matter the light-matter interaction described by the Rabi frequency, $\Omega_R = (\mathbf{D}\cdot\mathbf{e}_{\mathbf{k}})\mathcal{E}_{\mathbf{k}}/\hbar$, should be replaced by the effective Rabi frequency, $\Omega_{\mathrm{eff}}(t) = \Omega_R/[1 + i\pi W_a(\omega_{\mathbf{k}})J(0)]$[28] (see also Section 3).

In the site representation the photon emission rate of mode $\mathbf{k}$ obeys the equation

$$\frac{\partial}{\partial t}\langle a_{\mathbf{k}}^{\dagger}a_{\mathbf{k}}\rangle = \frac{i}{\hbar}\langle[-(\hat{\mathbf{D}}\cdot\hat{\mathbf{E}})_{\mathrm{eff}}, a_{\mathbf{k}}^{\dagger}a_{\mathbf{k}}]\rangle = 2\frac{\sqrt{2\pi\hbar\omega_{\mathbf{k}}}}{\hbar}\mathbf{D}\times\sum_m \mathrm{Re}\frac{\langle a_{\mathbf{k}}^{\dagger}\tilde{b}_m\rangle u_{\mathbf{k}}^*(\mathbf{r})}{1 - i\pi W_a^*(\omega_{\mathbf{k}})J(0)} \tag{35}$$

where in general the trace in this expression is over the vibrational as well as the field degrees of freedom, and we used relation $\mathbf{e}_{\mathbf{q}}\mathcal{E}_{\mathbf{q}}\exp(i\mathbf{q}\cdot\mathbf{r}) = i2\sqrt{2\pi\hbar\omega_{\mathbf{q}}}\,a_{\mathbf{q}}u_{\mathbf{q}}(\mathbf{r})$ between the amplitude of electric field, $\mathcal{E}_{\mathbf{q}}$, and the annihilation operator for mode $\mathbf{q}$, $a_{\mathbf{q}}$. Here $\tilde{b}_m = b_m\exp(i\omega_{\mathbf{k}}t)$ and $\langle b_m\rangle = \rho_{m,21}$ that should be calculated in the third order with respect to the light-matter interaction (see Figure 2).

Diagrams (1) and (2) of Figure 2 give contributions into $\langle\rho_{21}^{(3)}\rangle$. Adopting for a while the picture of fast vibrational relaxation when the equilibrium distribution into the excited electronic state has had time to be set during the lifetime of this state, one gets for the contribution described by the lower parts of these diagrams

$$\rho_{22}(\alpha) = \frac{n_2^{(2)}}{(2\pi K(0))^{1/2}}\exp\left[-\frac{(\alpha - \omega_{\mathrm{st}})^2}{2K(0)}\right] \tag{36}$$

where $n_2^{(2)} \ll 1$ is the population of excited electronic state 2 calculated in the second order with respect to electromagnetic field and $\omega_{\mathrm{st}} = \hbar K(0)/k_BT$ is the Stokes shift of the equilibrium absorption and luminescence spectra.

DOI: 10.1021/acs.jpcc.9b00582
J. Phys. Chem. C 2019, 123, 7366−7375

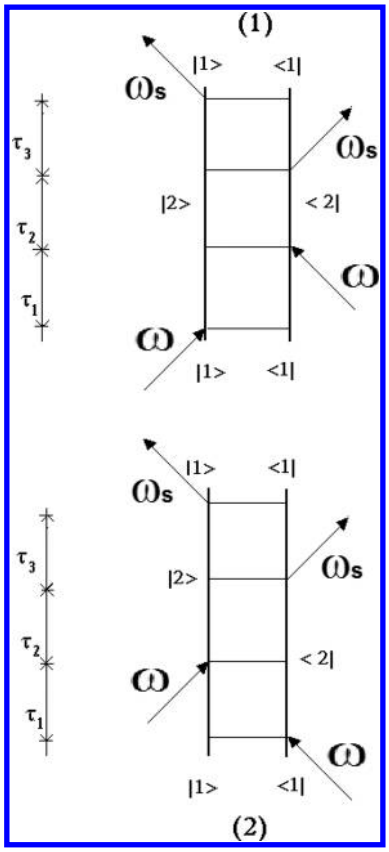

Figure 2. Double-sided Feynman diagrams for relaxed luminescence.

Consider equation for nondiagonal density matrix in the site representation related to the upper parts of diagrams (1) and (2) of Figure 2

$$\left[\frac{\partial}{\partial t} + i(\omega_{21} - \alpha) - L_{22}\right]\rho_{21}(\alpha, t) = \frac{i}{2\hbar}\mathbf{D}_{21}\cdot\mathbf{e}\mathcal{E}_{\mathbf{q}}\exp[i(\mathbf{q}\cdot\mathbf{r} - \omega_{\mathbf{q}}t)]\rho_{22}(\alpha) - iJ(0)\rho_{11}^{(0)}(\alpha)\int\rho_{21}(\alpha, t)\mathrm{d}\alpha \quad (37)$$

where operator

$$L_{22} = \tau_s^{-1}\left[1 + \frac{(\alpha - \omega_{st})\partial}{\partial(\alpha - \omega_{st})} + \frac{\sigma_{2s}\partial^2}{\partial(\alpha - \omega_{st})^2}\right]$$

describes the diffusion with respect to coordinate α in the excited electronic state. The latter and the presence of $\rho_{22}(\alpha)$ in the first term on the right-hand-side of eq 37 are distinctions of eq 37 from the corresponding equation related to absorption, eq 17. In contrast, the last term on the right-hand-side of eq 37 is the same as in the case of absorption (the presence of $\rho_{11}^{(0)}(\alpha)$). The fact is that this term describes the local field effects due to polarization of other molecules that are found in the main in the ground electronic state.

Equation 37 can be solved similar to the equation for absorption (see Section 1 of the Supporting Information). The homogeneous equation obtained from eq (37) can be reduced to eq (1) of the Supporting Information using notation $\alpha_2 = \alpha - \omega_{st}$ with the only difference that ω_{21} should be replaced by $\omega_{21} - \omega_{st}$. Then we obtain for the line shape of a monomer fluorescence

$$W_f(\omega_{\mathbf{k}}) = \frac{1}{\pi}\int_0^\infty \exp[i(\omega_{\mathbf{k}} - \omega_{21} + \omega_{st})t + g_s(t)]\mathrm{d}t \quad (38)$$

instead of eq (5) of the Supporting Information, and

$$W_f(\omega_{\mathbf{k}}) = \frac{\tau_s}{\pi}\frac{\Phi(1, 1 + x_f; K(0)\tau_s^2)}{x_f} \quad (39)$$

instead of eq 26, where $x_f = K(0)\tau_s^2 + i\tau_s(\omega_{21} - \omega_{st} - \omega_{\mathbf{k}})$.

When one includes also HFOA intramolecular vibrations (see Section 2 of the Supporting Information), the formula becomes

$$W_f(\omega_{\mathbf{k}}) = \frac{\tau_s}{\pi}\exp(-S_0\coth\theta_0)\sum_{l=-\infty}^{\infty} I_l\left(\frac{S_0}{\sinh\theta_0}\right) \times \exp(l\theta_0)\frac{\Phi(1, 1 + x_{fl}; K(0)\tau_s^2)}{x_{fl}} \quad (40)$$

where $x_{fl} = K(0)\tau_s^2 + i\tau_s(\omega_{21} - \omega_{st} - \omega_{\mathbf{k}} - l\omega_0)$. For $\theta_0 \gg 1$ we obtain

$$W_f(\omega_{\mathbf{k}}) = \frac{\tau_s}{\pi}\exp(-S_0)\sum_{l=0}^{\infty}\frac{S_0^l}{l!}\frac{\Phi(1, 1 + x_{fl}; K(0)\tau_s^2)}{x_{fl}} \quad (41)$$

Then we get for $\langle\tilde{b}_m\rangle = \langle\tilde{\rho}_{21}^{(3)}\rangle = \langle\rho_{21}^{(3)}\rangle\exp(i\omega_{\mathbf{k}}t)$

$$\langle\tilde{b}_m\rangle = -\frac{1}{\hbar}\sqrt{2\pi\hbar\omega_{\mathbf{k}}}\,a_{\mathbf{k}}\mathbf{D}_{21}\cdot u_{\mathbf{k}}(\mathbf{r})n_2^{(2)}\frac{\pi W_f(\omega_{\mathbf{k}})}{1 + i\pi J(0)W_a(\omega_{\mathbf{k}})} \quad (42)$$

Substituting eq 42 into eq 35, we obtain

$$\frac{\partial}{\partial t}\langle a_{\mathbf{k}}^\dagger a_{\mathbf{k}}\rangle = -\frac{4\pi^2}{\hbar^2 V}\hbar\omega_{\mathbf{k}}(\mathbf{D}_{12}\cdot\mathbf{e}_{\mathbf{k}}) \times \sum_m n_2^{(2)}\mathrm{Re}\frac{\langle a_{\mathbf{k}}^\dagger a_{\mathbf{k}}\rangle(\mathbf{D}_{21}\cdot\mathbf{e}_{\mathbf{k}})W_f(\omega_{\mathbf{k}})}{|1 + i\pi W_a(\omega_{\mathbf{k}})J(0)|^2} \quad (43)$$

where the fluorescence line shape of an exciton is given by

$$F_{\mathrm{exc},f}(\omega_{\mathbf{k}}) = \mathrm{Re}\frac{W_f(\omega_{\mathbf{k}})}{|1 + i\pi W_a(\omega_{\mathbf{k}})J(0)|^2} \quad (44)$$

and

$$n_2^{(2)} = \langle b_m^\dagger b_m\rangle^{(2)} \quad (45)$$

In deriving eq 43 we neglected the correlation between fluorescence photons and the medium polarization. Therefore, eq 43 describes the exciton luminescence. The polariton luminescence can be obtained in terms of the expectation values of $\langle a_{\mathbf{k}}^\dagger a_{\mathbf{k}'}\rangle$, $\langle a_{\mathbf{k}}^\dagger\tilde{b}_m\rangle$, $\langle\tilde{b}_m^\dagger\tilde{b}_n\rangle$, etc.,[47] satisfying coupled equations of motion and will be considered elsewhere.

Note that the exciton luminescence, eq 44, and absorption

$$F_{\mathrm{exc},a}(\omega_{\mathbf{k}}) = \mathrm{Re}\frac{W_a(\omega_{\mathbf{k}})}{1 + i\pi W_a(\omega_{\mathbf{k}})J(0)} = \mathrm{Re}\frac{W_a(\omega_{\mathbf{k}})}{|1 + i\pi W_a(\omega_{\mathbf{k}})J(0)|^2} \quad (46)$$

spectra obey Stepanov's law[11,30] if the corresponding monomer spectra obey this relation. Indeed, if $\mathrm{Re}W_f(\omega_{\mathbf{k}}) = \mathrm{Re}W_a(\omega_{\mathbf{k}}) \times$

DOI: 10.1021/acs.jpcc.9b00582
J. Phys. Chem. C 2019, 123, 7366−7375

$\exp[-\hbar(\omega_{\mathbf{k}}-\omega_{el})/k_BT]$, where $\omega_{el} = (E_2 - E_1)/\hbar$ is the frequency of a purely electronic transition, then

$$F_{exc,f}(\omega_{\mathbf{k}}) = F_{exc,a}(\omega_{\mathbf{k}})\exp[-\hbar(\omega_{\mathbf{k}} - \omega_{el})/k_BT] \quad (47)$$

Figure 3 shows absorption and fluorescence spectra of a J-aggregate calculated using eqs 46 and (44), respectively. The

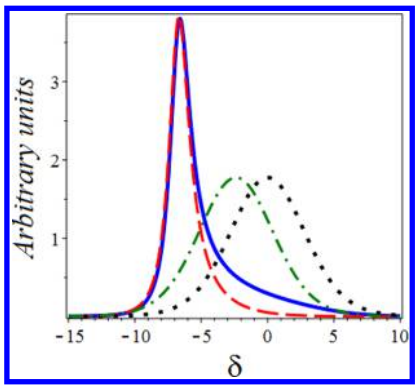

Figure 3. Absorption (solid) and relaxed luminescence (dash) spectra of a J-aggregate for $\sqrt{K(0)}\,\tau_s = 3.16$, $\tau_s = 1 \times 10^{-13}$ s and $-J(0)\tau_s = 5$. The monomer absorption (dots) and luminescence (dash-dot) are shown for comparison.

monomer spectra $W_a(\omega_{\mathbf{k}})$ and $W_f(\omega_{\mathbf{k}})$ were calculated using eqs 26 and (39), respectively. One can see that the position of the luminescence spectrum is determined in the main by the pole of the denominator on the right-hand side of eq 44 that is approximately the same as for aborption. That is why the positions of the J-aggregate luminescence and absorption spectra concide, according to experiment, in spite of the Stokes shift of the corresponding monomer spectra (see Figure 3). We emphasize that both narrowing the J-aggregate spectra and diminishing their Stokes shift with respect to those of a monomer covered by our non-Markovian theory cannot be described by the model of a single HFOA vibration.[25,27] We shall apply the theory of this section to H-aggregates below.

4.1. Exciton Luminescence in *k*-Space. Consider an exciton luminescence in the **k**-space. Using eq 45, and bearing in mind that $\sum_m b_m^\dagger b_m = \sum_{\mathbf{k}'} b_{\mathbf{k}}^\dagger b_{\mathbf{k}'}$ and that the translational symmetry of a perfect bulk crystal implies that excitons of wave vector **k** can only couple to electromagnetic waves of the same wave vector, we get from eq 43

$$\frac{\partial}{\partial t}\langle a_{\mathbf{k}}^\dagger a_{\mathbf{k}}\rangle = -\frac{4\pi^2}{\hbar^2 V}\hbar\omega_{\mathbf{k}}(\mathbf{D}_{12}\cdot\mathbf{e}_{\mathbf{k}})\langle b_{\mathbf{k}}^\dagger b_{\mathbf{k}}\rangle^{(2)} \times \mathrm{Re}\frac{\langle a_{\mathbf{k}}^\dagger a_{\mathbf{k}}\rangle(\mathbf{D}_{21}\cdot\mathbf{e}_{\mathbf{k}})W_f(\omega_{\mathbf{k}})}{|1 + i\pi W_a(\omega_{\mathbf{k}})J(\mathbf{k})|^2} \quad (48)$$

Let us suppose a thermal equilibrium in the **k**-space

$$\langle b_{\mathbf{k}}^\dagger b_{\mathbf{k}}\rangle^{(2)} \approx \frac{\exp[-J(\mathbf{k})/k_BT]}{\sum_{\mathbf{k}}\exp[-J(\mathbf{k})/k_BT]} \quad (49)$$

and assume for simplicity that the excitons have an isotropic effective mass, eq 33. For positive effective mass $J(\mathbf{k})$ may be replaced by $J(0)$ like before, and we arrive to the result obtained in the site representation. In contrast, for negative effective mass, $J(\mathbf{k}) \approx J(\mathbf{k}_{lum})$, where $\mathbf{k}_{lum}$ corresponds to the minimum of $J(\mathbf{k})$. In that case one can expect an additional red shift of the luminescence spectrum with respect to the vibrational Stokes shift ω_{st}.

5. APPLICATION TO EXCITON-POLARITON EXPERIMENT IN NANOFIBER

In this section we apply the theory developed above to the experiment on fraction of a millimeter propagation of EPs in photoexcited fiber-shaped H-aggregates of TC dye at room temperature[3] bearing in mind the correspondence between manifestation of electron-vibrational interaction in monomers, molecular aggregates, and EP dispersion in nanofibers.

Figure 4 shows the experimental absorption line shape of TC monomer solution prepared by dissolving TC dye in

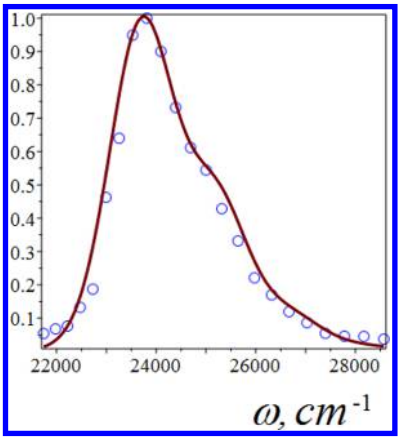

Figure 4. Experimental absorption line shape of TC monomer solution prepared by dissolving TC dye in methanol[1] (○) and its fitting by $\mathrm{Re}W_a$, eq 28, (solid line).

methanol[1] and its fitting by $\mathrm{Re}W_a$, eq 28 for $\omega_{21} = 23\,700$ cm^{-1}, $1/\tau_s = 75$ cm^{-1}, $\omega_0\tau_s = 20$, $S_0 = 0.454$, $K(0)\tau_s^2 = 80$.

Using the last parameters, we calculated the aggregate absorption and photoluminescence spectra according to formulas 46 and (44), respectively, shown in Figure 5. Good agreement between theoretical and experimental spectra is observed with the value of parameter $J(0)\tau_s = 7$ obtained by comparison between experimental and theoretical curves. Dimensionless parameter of the Stokes shift is equal to $\omega_{st}\tau_s = \hbar K(0)\tau_s^2/(k_BT\tau_s) = 28.6$ for room temperature ($k_BT/\hbar = 210$ cm^{-1}). We did not make additional fitting, since experimental spectra of TC aggregates and monomers were measured in different solvents[1] (see caption to Figure 5).

It might be well to point out that both absorption and luminescence H-aggregate spectra were obtained using only one additional parameter $J(0)\tau_s = 7$ with respect to those found by fitting the absorption monomer spectrum. This speaks in favor of the proposed physical model of forming the aggregate spectra.

The description of the aggregate spectra obtained above enables us to get the dielectric function, eq 32, and find the transverse eigenmodes of the medium from the dispersion equation

$$c^2k^2(\omega_{\mathbf{k}}) = \omega_{\mathbf{k}}{}^2\varepsilon(\mathbf{k}, \omega_{\mathbf{k}}) \quad (50)$$

Bearing in mind discussion just after eq 32, we take the exciton resonances at $J(0)$ (so-called $\mathbf{k} = 0$ selection rule[10]), so that we shall use $\varepsilon(0,\omega) \equiv \varepsilon(\omega)$ in our simulations of EP dispesion. Inclusion of spatial dispersion in ref 3 to account for line broadening arose from the use a simple Lorentz model that

DOI: 10.1021/acs.jpcc.9b00582
J. Phys. Chem. C 2019, 123, 7366−7375

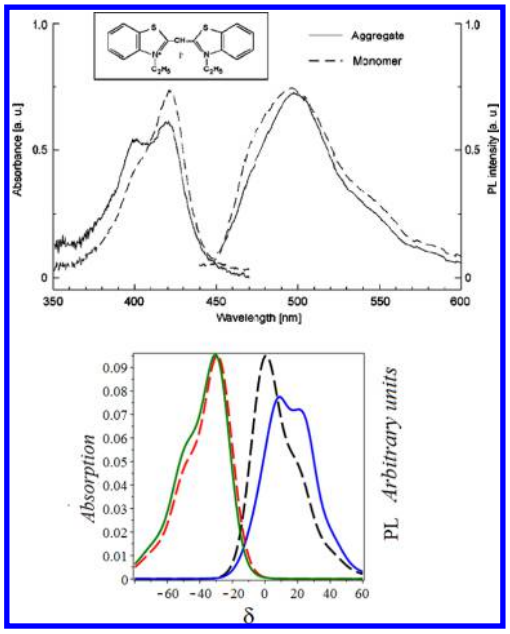

Figure 5. Experimental absorption and photoluminescence spectra of TC aggregates and monomers[1] (top) and theoretical description of aggregate absorption (in terms of τ_s/π) and photoluminescence (arbitrary units) (bottom). In the top solid curve represents spectra of the aqueous solution containing TC aggregates; dashed curve represents spectra of a monomer solution prepared by dissolving TC dye in methanol. In the bottom solid curves represent the aggregate spectra; dashed curves represent spectra of a monomer. Dimensionless parameter $\delta = \tau_s(\omega - \omega_{21})$ increases when the wavelength decreases.

does not take electron-vibrational effects into consideration. Because the fiber in ref 3 had a rectangular cross section with width of 400−700 nm ($\sim\lambda$) and height of 100−200 nm ($\ll\lambda$), the energy of light guided in the nanofiber was given by

$$\hbar\omega = \sqrt{\hbar^2 c^2 k_{\|}^{\ 2} + E_C^{\ 2}}/n(\omega) \tag{51}$$

where $\mathbf{k}_{\|}$ is the wave vector parallel to the fiber, and $E_C = \hbar c\pi/d = 1$ eV for $d = 600$ nm is the cutoff energy. Combining eqs 50 and (51), we get

$$c^2 k_{\|}^{\ 2} = \omega^2\varepsilon(\omega) - \frac{E_C^{\ 2}}{\hbar^2} \tag{52}$$

Let us analyze eq 52, where the dielectric function $\varepsilon(0,\omega) \equiv \varepsilon(\omega)$ is determined by eq 32 for $J(\mathbf{k}) = J(0)$. In ref 28 we considered rather the transverse eigenmodes of the medium, eq 50, than the nanofiber modes with wave vector $\mathbf{k}_{\|}$. The parameters of the aggregate spectrum were found above. To satisfy eq 52, the wavenumber $k_{\|}$ should be complex $k_{\|} = k'_{\|} + ik''_{\|}$. Then using eq 52, we get for the real and imaginary part of $k_{\|}$

$$k'_{\|}\frac{c}{n_0} = \omega\mathrm{Re}\sqrt{\left[1 - \frac{(E_C/\hbar)^2}{\omega^2\varepsilon_0}\right] + iq\pi\frac{W_a(\omega)}{1 + i\pi W_a(\omega)J(0)}} \tag{53}$$

and

$$k''_{\|}\frac{c}{n_0} = \omega\mathrm{Im}\sqrt{\left[1 - \frac{(E_C/\hbar)^2}{\omega^2\varepsilon_0}\right] + iq\pi\frac{W_a(\omega)}{1 + i\pi W_a(\omega)J(0)}} \tag{54}$$

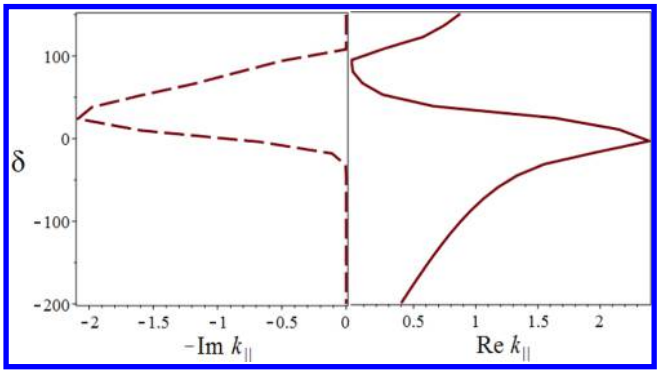

Figure 6. Frenkel EP dispersion for real (solid line) and imaginary (dashed line) part of the wavenumber $k_{\|}$ calculated with eqs 53 and (54), respectively, when $q\tau_s = 84$.[28] Other parameters are identical to those of the bottom of Figure 5.

respectively, where $q = 4\pi\frac{N\mathbf{D}_{12}\mathbf{D}_{21}}{\hbar}$. Figure 6 shows the Frenkel EP dispersion calculated using eqs 53 and (54). The polariton dispersion shows the leaky part in the splitting range between lower and upper polariton branches. The fluorescence spectrum of a nanofiber was in the range of ∼2.5 eV,[3] where in the main $\mathrm{Im}k_{\|} \approx 0$. In addition, the fluorescence spectrum was out of the splitting range under discussion and corresponded to the lower polariton branch due to excitation at $\lambda = 405$ nm below the upper polariton branch. However, if the excitation was at upper polariton branch, photoluminescence from it would be unlikely due to the presence of absorption ($\mathrm{Im}k_{\|} \neq 0$) in the range of upper polariton branch (see Figure 6). In contrast, EP emission in materials with narrow absoption lines (J-aggregates) show photoluminescence from both upper and lower polariton branches.[5,48] It is worth noting that this and other conclusions related to the EP dispersion are based on the correspondence between manifestation of electron-vibrational interaction in monomers, molecular aggregates, and EP dispersion in nanofibers. This correspondence is of particular importance when the bandwidth of the imaginary part of the wave vector is of the same order of magnitude as the splitting range between lower and upper polariton branches (see Figure 6).

In this work we restricted ourselves to the exciton luminescence, Section 4, due to factorization of the term $\langle a_{\mathbf{k}}^{\dagger}\tilde{b}_m\rangle$ on the right-hand side of eq 35 adopted in moving from eq 35 to eq 43. The factorization enabled us to split the corresponding term on the right-hand side of eq 43 into the product of field intensity, $\langle a_{\mathbf{k}}^{\dagger}a_{\mathbf{k}}\rangle$, and the material term $\sim n_2^{(2)}F_{\mathrm{exc},f}(\omega_{\mathbf{k}})$, where $F_{\mathrm{exc},f}(\omega_{\mathbf{k}})$ is the fluorescence line shape of an exciton, eq 44. However, the approach developed in Section 4 can be extended to the polariton luminescence that can be obtained in terms of the expectation values of $\langle a_{\mathbf{k}}^{\dagger}a_{\mathbf{k}'}\rangle$, $\langle a_{\mathbf{k}}^{\dagger}\tilde{b}_m\rangle$, $\langle \tilde{b}_m^{\dagger}\tilde{b}_n\rangle$, etc.[47] satisfying coupled equations of motion. In contrast to the results described in ref 47, our coupled equations of motion will include non-Markovian relaxation making their solution more complex. This will be done elsewhere.

DOI: 10.1021/acs.jpcc.9b00582
J. Phys. Chem. C 2019, 123, 7366−7375

6. CONCLUSION

In this work we have developed a model to account for electron-vibrational effects on absorption and luminescence of molecular aggregates, and EPs in nanofibers. The model generalizes the mean-field electron-vibrational theory developed by us earlier to the systems with spatial symmetry, exciton luminescence, and the EPs with spatial dispersion. The exciton luminescence and absorption spectra in our mean-field theory obey Stepanov's law.[11,30] Among other things, our theory describes both narrowing the J-aggregate absorption and luminescence spectra and diminishing the Stokes shift between them with respect to that of a monomer. The correspondence between manifestation of electron-vibrational interaction in monomers, molecular aggregates, and EP dispersion in nanofibers is obtained by introducing the aggregate line-shape functions in terms of the monomer line-shape functions. With the same description of material parameters we have calculated both the absorption and luminescence of molecular aggregates and the EP dispersion in nanofibers. We obtained good agreement between theoretical and experimental absorption and luminescence spectra of both monomers and H-aggregates. We emphasize that both absorption and luminescence H-aggregate spectra were obtained using only one additional parameter with respect to those found by fitting the absorption monomer spectrum. This speaks in favor of the proposed physical model of forming the aggregate spectra. We have applied the theory to experiment on fraction of a millimeter propagation of Frenkel EPs in photoexcited fiber-shaped H-aggregates of TC dye at room temperature[3] bearing in mind the correspondence between manifestation of electron-vibrational interaction in monomers, molecular aggregates, and EP dispersion in nanofibers.

We have also discussed the extension of our approach to the description of polariton luminescence. This will be done elsewhere.

The theory can be also applied to Frenkel EPs in organic microcavities,[27,49] to plexcitonics,[50] and the problems related to optics of exciton−plasmon nanomaterials,[51,52] where the rovibrational structure of diatomic molecules was recently included.[53] In contrast, in our paper we consider a model for aggregates of large organic molecules.

ASSOCIATED CONTENT

Supporting Information

The Supporting Information is available free of charge on the ACS Publications website at DOI: 10.1021/acs.jpcc.9b00582.

Calculation of the contribution of LFOA vibrations to monomer spectrum, including HFOA intramolecular vibrations (PDF)

AUTHOR INFORMATION

Corresponding Author

*E-mail: fainberg@hit.ac.il.

ORCID

Boris D. Fainberg: 0000-0003-3596-6326

Notes

The author declares no competing financial interest.

ACKNOWLEDGMENTS

This work was supported by the Ministry of Science & Technology of Israel (Grant No. 79518). I thank G. Rosenman and B. Apter for useful discussions.

REFERENCES

(1) Takazawa, K.; Kitahama, Y.; Kimura, Y.; Kido, G. Optical Waveguide Self-Assembled from Organic Dye Molecules in Solution. *Nano Lett.* **2005**, *5*, 1293−1296.

(2) Takazawa, K. Waveguiding Properties of Fiber-Shaped Aggregates Self-Assembled from Thiacyanine Dye Molecules. *J. Phys. Chem. C* **2007**, *111*, 8671−8676.

(3) Takazawa, K.; Inoue, J.; Mitsuishi, K.; Takamasu, T. Fraction of a Millimeter Propagation of Exciton Polaritons in Photoexcited Nano fibers of Organic Dye. *Phys. Rev. Lett.* **2010**, *105*, 067401.

(4) Takazawa, K.; Inoue, J.; Mitsuishi, K.; Kuroda, T. Ultracompact Asymmetric Mach-Zehnder Interferometers with High Visibility Constructed from Exciton Polariton Waveguides of Organic Dye Nanofibers. *Adv. Funct. Mater.* **2013**, *23*, 839−845.

(5) Ellenbogen, T.; Crozier, K. B. Exciton-Polariton Emission from Organic Semiconductor Optical Waveguides. *Phys. Rev. B: Condens. Matter Mater. Phys.* **2011**, *84*, 161304.

(6) Gentile, M. J.; Nunez-Sanchez, S.; Barnes, W. L. Optical Field-Enhancement and Subwavelength Field-Confinement Using Excitonic Nanostructures. *Nano Lett.* **2014**, *14*, 2339−2344.

(7) Liao, Q.; Xu, Z.; Zhong, X.; Dang, W.; Shi, Q.; Zhang, C.; Weng, Y.; Li, Z.; Fu, H. An Organic Nanowire Waveguide Exciton-Polariton Sub-Microlaser and Its Photonic Application. *J. Mater. Chem. C* **2014**, *2*, 2773−2778.

(8) Gather, M. C.; Yun, S. H. Single-Cell BiologicalLasers. *Nat. Photonics* **2011**, *5*, 406−410.

(9) Dietrich, C. P.; Steude, A.; Tropf, L.; Schubert, M.; Kronenberg, N. M.; Ostermann, K.; Hofling, S.; Gather, M. C. An Exciton-Polariton Laser Based on Biologically Produced Fluorescent Protein. *Sci. Adv.* **2016**, *2*, e1600666.

(10) Knoester, J.; Agranovich, V. M. Frenkel and Charge-Transfer Excitons in Organic Solids. In *Thin Films and Nanostructures: Electronic Excitations in Organic Based Nanostructures;* Agranovich, V. M., Bassani, G. F., Eds.; Elsevier Academic Press: Amsterdam, 2003; Vol. *31*.

(11) Agranovich, V. M. *Excitations in Organic Solids;* Oxford University Press: New York, 2009.

(12) Handelman, A.; Lapshina, N.; Apter, B.; Rosenman, G. Peptide Integrated Optics. *Adv. Mater.* **2018**, *30*, 1705776.

(13) Apter, B.; Lapshina, N.; Handelman, A.; Fainberg, B. D.; Rosenman, G. Peptide Nanophotonics: From Optical Waveguiding to Precise Medicine and Implantable Biochips. *Small* **2018**, 1801147.

(14) Lapshina, N.; Shishkin, I.; Nandi, R.; Noskov, R. E.; Barhom, H.; Joseph, S.; Apter, B.; Ellenbogen, T.; Natan, A.; Ginzburg, P.; et al. Bioinspired Amyloid Nanodots with Visible Fluorescence. *Adv. Opt. Mater.* **2018**, 1801400.

(15) Joseph, S. K.; Kuritz, N.; Yahel, N.; Lapshina, N.; Rosenman, G.; Natan, A. Proton-transfer induced fluorescence in self-assembled short peptides. *J. Phys. Chem. A* **2019**, *13*.

(16) Hopfield, J. J. Theory of the Contribution of Excitons to the Complex Dielectric Constant of Crystals. *Phys. Rev.* **1958**, *112*, 1555−1567.

(17) Knoester, J.; Mukamel, S. Transient Gratings, Four-Wave Mixing and Polariton Effects in Nonlinear Optics. *Phys. Rep.* **1991**, *205*, 1−58.

(18) Zoubi, H. Collective Interactions in an Array of Atoms Coupled to a Nanophotonic Waveguide. *Phys. Rev. A: At., Mol., Opt. Phys.* **2014**, *89*, 043831.

(19) Plumhof, J. D.; Stoferle, T.; Mai, L.; Scherf, U.; Mahrt, R. F. Room-Temperature Bose-Einstein Condensation of Cavity Exciton-Polaritons in a Polymer. *Nat. Mater.* **2014**, *13*, 247−252.

(20) Lerario, G.; Fieramosca, A.; Barachati, F.; Ballarini, D.; Daskalakis, K. S.; Dominici, L.; De Giorgi, M.; Maier, S. A.; Gigli,

DOI: 10.1021/acs.jpcc.9b00582
J. Phys. Chem. C 2019, 123, 7366−7375

G.; Kena-Cohen, S.; et al. Room-Temperature Superfluidity in a Polariton Condensate. *Nat. Phys.* **2017**, *13*, 837−841.
(21) Karzig, T.; Bardyn, C.-E.; Lindner, N. H.; Refael, G. Topological Polaritons. *Phys. Rev. X* **2015**, *5*, 031001.
(22) Nalitov, A. V.; Solnyshkov, D. D.; Malpuech, G. Polariton Z Topological Insulator. *Phys. Rev. Lett.* **2015**, *114*, 161413.
(23) Klembt, S.; Harder, T. H.; Egorov, O. A.; Winkler, K.; Ge, R.; Bandres, M. A.; Emmerling, M.; Worschech, L.; Liew, T. C. H.; Segev, M.; et al. Exciton-Polariton Topological Insulator. *Nature* **2018**, *562*, 552−556.
(24) Mukamel, S.; Deng, Z.; Grad, J. Dielectric Response, Nonlinear-Optical Processes, and the Bloch-Maxwell Equations for Polarizable Fluids. *J. Opt. Soc. Am. B* **1988**, *5*, 804−816.
(25) Fontanesi, L.; Mazza, L.; La Rocca, G. C. Organic-Based Microcavities with Vibronic Progressions: Linear Spectroscopy. *Phys. Rev. B: Condens. Matter Mater. Phys.* **2009**, *80*, 235313.
(26) Toyozawa, Y. On the Dynamical Behavior of an Exciton. *Progr. Theor. Phys. Suppl.* **1959**, *12*, 111−140.
(27) Mazza, L.; Fontanesi, L.; La Rocca, G. C. Organic-Based Microcavities with Vibronic Progressions: Photoluminescence. *Phys. Rev. B: Condens. Matter Mater. Phys.* **2009**, *80*, 235314.
(28) Fainberg, B. D. Mean-Field Electron-Vibrational Theory of Collective Effects in Photonic Organic Materials. Long-Range Frenkel Exciton Polaritons in Nanofibers of Organic Dye. *AIP Adv.* **2018**, *8*, 075314.
(29) Eisfeld, A.; Briggs, J. S. Absorption Spectra of Quantum Aggregates Interacting via Long-Range Forces. *Phys. Rev. Lett.* **2006**, *96*, 113003.
(30) Stepanov, B. I. Universal Relation Between Absorption and Luminescence Spectra of Complex Molecules. *Dokl. Akad. Nauk SSSR* **1957**, *112*, 839−841.
(31) Davydov, A. S. *Theory of Molecular Excitons;* Plenum: New York, 1971.
(32) Mukamel, S. *Principles of Nonlinear Optical Spectroscopy;* Oxford University Press: New York, 1995.
(33) Fainberg, B. D. Ultrafast Dynamics and Non-Markovian Processes in Four-Photon Spectroscopy. In *Advances in Multiphoton Processes and Spectroscopy;* Lin, S. H., Villaeys, A. A., Fujimura, Y., Eds.; World Scientific: Singapore, 2003; Vol. *15*.
(34) Fainberg. Theory of the Non-Stationary Spectroscopy of Ultrafast Vibronic Relaxations in Molecular Systems on the Basis of Degenerate Four-Wave Mixing. B. D. *Opt. Spectrosc.* **1990**, *68*, 305−309.
(35) Fainberg, B. Learning About Non-Markovian Effects byDegenerate Four-Wave-Mixing Processes. *Phys. Rev. A: At., Mol., Opt. Phys.* **1993**, *48*, 849−850.
(36) Fainberg, B. D. Non-Linear Polarization and Spectroscopyof Vibronic Transitions in the Field of Intensive Ultrashort Pulses. *Chem. Phys.* **1990**, *148*, 33−45.
(37) Fainberg, B. D. Nonperturbative Analytic Approach to Interaction of Intense Ultrashort Chirped Pulses with Molecules in Solution: Picture of "Moving" Potentials. *J. Chem. Phys.* **1998**, *109*, 4523−4532.
(38) Fainberg, B. D.; Levinsky, B. Stimulated Raman Adiabatic Passage in a Dense Medium. *Adv. Phys. Chem.* **2010**, *2010*, 798419.
(39) Haug, H.; Koch, S. W. *Quantum Theory of the Optical and Electronic Properties of Semiconductors;* World Scientific: Singapore, 2001.
(40) Rautian, S. G.; Sobel'man, I. I. The Effect of Collisions on the Doppler Broadening of Spectral Lines. *Soviet Physics Uspekhi* **1967**, *9*, 701−716. [Usp. Fiz. Nauk 90, 209−238 (1966)].
(41) Fainberg, B. D.; Narbaev, V. Chirped Pulse Excitationin Condensed Phase Involving Intramolecular Modes Studied by Double-Sided Feynman Diagrams for Fast Electronic Dephasing. *J. Chem. Phys.* **2000**, *113*, 8113−8124.
(42) Fainberg, B. D.; Narbaev, V. Chirped Pulse Excitationin Condensed Phase Involving Intramolecular Modes. II. Absorption Spectrum. *J. Chem. Phys.* **2002**, *116*, 4530−4541.
(43) Abramowitz, M.; Stegun, I. *Handbook on Mathematical Functions;* Dover: New York, 1964.
(44) Fainberg, B. D. Stochastic Theory of the Spectroscopy of Optical Transitions Based on Four-Photon Resonance Interaction and Photo-Echo-Type Effects. *Opt. Spectrosc.* **1985**, *58*, 323−328.
(45) Litinskaya, M. Exciton Polariton Kinematic Interaction in Crystalline Organic Microcavities. *Phys. Rev. B: Condens. Matter Mater. Phys.* **2008**, *77*, 155325.
(46) Yee, T. K.; Gustafson, T. K. Diagrammatic Analysis of the Density Operator for Nonlinear Optical Calculations: Pulsed and CW Responses. *Phys. Rev. A: At., Mol., Opt. Phys.* **1978**, *18*, 1597−1617.
(47) Chovan, J.; Perakis, I. E.; Ceccarelli, S.; Lidzey, D. G. Controlling the Interactions Between Polaritons and Molecular Vibrations in Strongly Coupled Organic Semiconductor Microcavities. *Phys. Rev. B: Condens. Matter Mater. Phys.* **2008**, *78*, 045320.
(48) Schwartz, T.; Hutchison, J. A.; Leonard, J.; Genet, C.; Haacke, S.; Ebbesen, T. W. Polariton Dynamics under Strong Light-Molecule Coupling. *ChemPhysChem* **2013**, *14*, 125−131.
(49) Litinskaya, M.; Reineker, P.; Agranovich, V. M. Exciton-Polaritons in Organic Microcavities. *J. Lumin.* **2006**, *119−120*, 277−282.
(50) Halas, N. J.; Lal, S.; Chang, W.-S.; Link, S.; Nordlander, P. Quantum Plexcitonics: Strongly Interacting Plasmons and Excitons. *Chem. Rev.* **2011**, *111*, 3913−3961.
(51) White, A. J.; Fainberg, B. D.; Galperin, M. Collective Plasmon-Molecule Excitations in Nanojunctions: Quantum Consideration. *J. Phys. Chem. Lett.* **2012**, *3*, 2738−2743.
(52) Sukharev, M.; Nitzan, A. Optics of Exciton-Plasmon Nanomaterials. *J. Phys.: Condens. Matter* **2017**, *29*, 443003.
(53) Sukharev, M.; Charron, E. Molecular Plasmonics: The Role of Rovibrational Molecular States in Exciton-Plasmon Materials under Strong-Coupling Conditions. *Phys. Rev. B: Condens. Matter Mater. Phys.* **2017**, *95*, 115406.

DOI: 10.1021/acs.jpcc.9b00582
J. Phys. Chem. C 2019, 123, 7366−7375